



Oral Vaccination with Replication-Competent Adenovirus in Mice Reveals Dissemination of the Viral Vaccine beyond the Gastrointestinal Tract

Emeline Goffin,^a Justine Javaux,^a Eric Destexhe,^b Carla D. Pretto,^c  Katherine R. Spindler,^c Bénédicte Machiels,^a  Laurent Gillet^a

^aLaboratory of Immunology and Vaccinology, Department of Infectious Diseases Faculty of Veterinary Medicine, FARAH, University of Liège, Liège, Belgium

^bGSK, Rixensart, Belgium

^cDepartment of Microbiology and Immunology, University of Michigan, Ann Arbor, Michigan, USA

ABSTRACT Since the 1970s, replication-competent human adenoviruses 4 and 7 have been used as oral vaccines to protect U.S. soldiers against the severe respiratory diseases caused by these viruses. These vaccines are thought to establish a digestive tract infection conferring protection against respiratory challenge through antibodies. The success of these vaccines makes replication-competent adenoviruses attractive candidates for use as oral vaccine vectors. However, the inability of human adenoviruses to replicate efficiently in laboratory animals has hampered the study of such vectors. Here, we used mouse adenovirus type 1 (MAV-1) in mice to study oral replication-competent adenovirus-based vaccines. We show that MAV-1 oral administration provides protection that recapitulates the protection against homologous respiratory challenge observed with adenovirus 4 and 7 vaccines. Moreover, live oral MAV-1 vaccine better protected against a respiratory challenge than inactivated vaccines. This protection was linked not only with the presence of MAV-1-specific antibodies but also with a better recruitment of effector CD8 T cells. However, unexpectedly, we found that such oral replication-competent vaccine systemically spread all over the body. Our results therefore support the use of MAV-1 to study replication-competent oral adenovirus-based vaccines but also highlight the fact that those vaccines can disseminate widely in the body.

IMPORTANCE Replication-competent adenoviruses appear to be promising vectors for the development of oral vaccines in humans. However, the study and development of these vaccines suffer from the lack of any reliable animal model. In this study, mouse adenovirus type 1 was used to develop a small-animal model for oral replication-competent adenovirus vaccines. While this model reproduced in mice what is observed with human adenovirus oral vaccines, it also highlighted that oral immunization with such a replication-competent vaccine is associated with the systemic spread of the virus. This study is therefore of major importance for the future development of such vaccine platforms and their use in large human populations.

KEYWORDS adenovirus, mouse model, oral vaccination

Oral vaccination offers economical and logistical advantages compared to other delivery methods. In addition, mucosal administration of antigens could improve vaccine efficacy by inducing better responses at the site of entry of many pathogens (1). However, achieving a protective immune response through the oral route is still challenging (2–4). Indeed, in the intestine, which is constantly subjected to commensal bacteria and food antigens, immune responses are contained by potent regulatory mechanisms that prevent uncontrolled activation (5, 6). Therefore, oral vaccines require

Citation Goffin E, Javaux J, Destexhe E, Pretto CD, Spindler KR, Machiels B, Gillet L. 2019. Oral vaccination with replication-competent adenovirus in mice reveals dissemination of the viral vaccine beyond the gastrointestinal tract. *J Virol* 93:e00237-19. <https://doi.org/10.1128/JVI.00237-19>.

Editor Lawrence Banks, International Centre for Genetic Engineering and Biotechnology

Copyright © 2019 American Society for Microbiology. All Rights Reserved.

Address correspondence to Laurent Gillet, L.Gillet@uliege.be.

Received 12 February 2019

Accepted 13 April 2019

Accepted manuscript posted online 17 April 2019

Published 14 June 2019

efficient delivery systems to elicit effective immune responses. Adenovirus vectors have desirable features in that context (1).

Adenoviruses are nonenveloped with an icosahedral capsid containing a linear double-stranded DNA genome. Human adenoviruses cause acute pathologies, which are usually mild but which can be more severe in immunocompromised subjects (7). Despite the attractive properties of adenovirus vaccine vectors, including genome stability, growth to high titers, and efficient stimulation of innate and adaptive immunity (8), a major limitation to their use is the seroprevalence against many adenovirus types in human populations (9). However, mucosal administration would not be affected by preexisting immunity (10). Furthermore, in comparison with replication-defective vectors, replication-competent adenovirus vectors may have an enhanced ability to break immune tolerance mechanisms present in the gut mucosa (11). Countering the concern about the risks associated with replication-competent vectors (12), most epidemiological data have established the safety of replicative adenoviruses when they are administered orally. Indeed, since the 1970s, wild-type human adenovirus type 4 (Ad4) and Ad7 have been used as oral vaccines to protect members of the U.S. military from the severe acute respiratory diseases caused by these two viruses (13–17).

To date, these oral vaccines have been administered to more than 10 million U.S. military trainees, showing 95% efficacy and no reported significant adverse effects (16). In view of this success, replication-competent adenoviruses are promising vectors for the development of oral vaccine platforms (18–20). These replication-competent adenovirus vaccines are thought to induce a local, transient, and asymptomatic intestinal infection that elicits neutralizing antibodies in serum and subsequent protection against a respiratory challenge with the same viruses (15, 21). After immunization, a better recruitment of immune cells at other mucosal surfaces may also be possible, but this hypothesis has never been investigated (15).

The potential of replication-competent adenoviruses as vectors for heterologous immunization has been poorly explored to date (8, 22–24). The study and development of replication-competent adenovirus vectors are hampered by their high host specificity. In particular, human adenoviruses do not replicate efficiently in rodents. Respiratory infection has been achieved in cotton rat, Syrian hamster, and mouse models, but it requires very high doses (10^7 to 10^{10} PFU) (25–27). The use of a host that supports efficient viral replication is essential to study live vaccines under conditions that mimic their intended use in humans. Therefore, administration of mouse adenovirus type 1 (MAV-1) to mice is a relevant and useful model to study replication-competent adenovirus infection in its natural host (28–30). Moreover, MAV-1 intranasal infection elicits in C57BL/6 and BALB/c mice an interstitial pneumonitis that has been used as a model for human acute respiratory disease caused by human Ad4 and Ad7 (30–34).

In order to develop a model for evaluation of orally administered replication-competent adenovirus vaccines in mice, we characterized oral infection of BALB/c mice by MAV-1, and we evaluated the protection that oral administration of replication-competent MAV-1 confers against an intranasal challenge with the same virus.

RESULTS

MAV-1 oral infection is subclinical and gives rise to a virus-specific and neutralizing antibody response. To characterize MAV-1 oral infection, groups of 8-week-old female BALB/c mice were infected through the oral route (by the use of an esophageal feeding needle) with 10^4 50% tissue culture infective doses (TCID₅₀) of MAV-1 and then euthanized at day 3, 7, 14, or 21 postinfection (p.i.) (Fig. 1a). No specific clinical signs (data not shown) or weight loss (Fig. 1b) were observed in MAV-1-infected mice compared to mock-infected mice at any time point. At the postmortem examination, the only differences seen were enlarged mesenteric lymph nodes and Peyer's patches (data not shown). However, quantitative PCR (qPCR) of feces revealed sporadic shedding of the virus at least up to 21 days p.i. (Fig. 1c), suggesting local replication in the gut. Since human adenovirus oral vaccines produce a specific and neutralizing

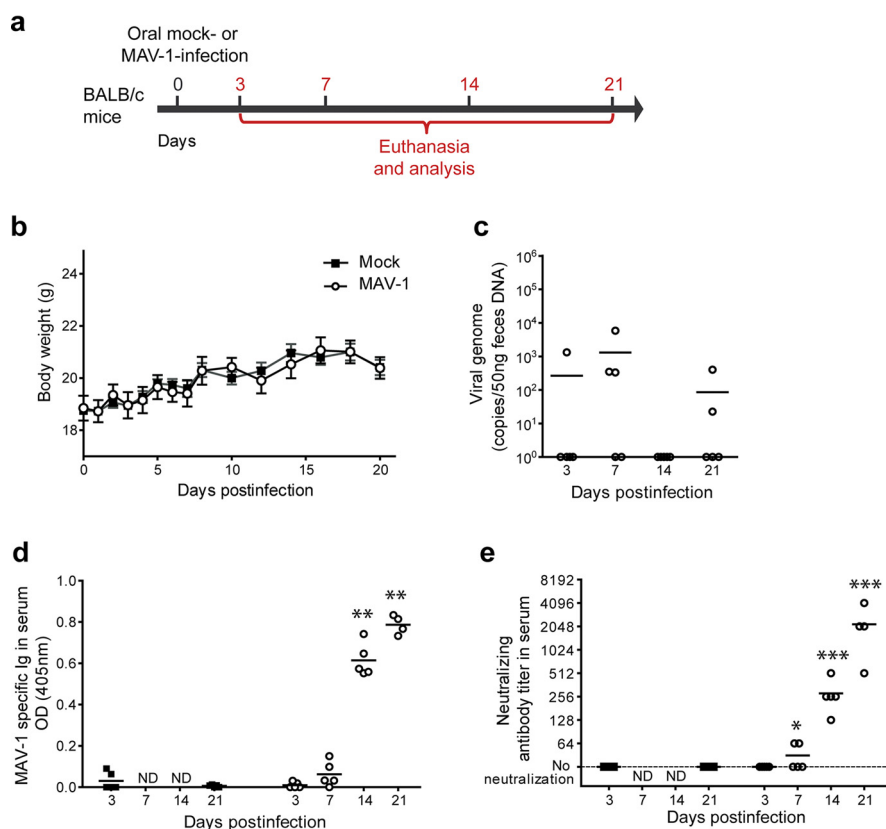


FIG 1 Characterization of MAV-1 oral infection in BALB/c mice. (a) Eight-week-old female BALB/c mice were orally infected with 10^4 TCID₅₀ of MAV-1 or PBS (mock) and euthanized at day 3, 7, 14, or 21 p.i. for analysis ($n = 5$ mice in each group). The numbers above the arrow indicate the day postinfection. (b) Weight of mice. (c) MAV-1 genome copy numbers in feces. (d) MAV-1-specific antibodies. OD, optical density. (e) MAV-1-neutralizing antibody titers. The data presented are either the means for 5 mice \pm SEM (b) or individual data and means (c to e). Pooled data from naive mice at days 3 and 21 provided the negative control ($n = 10$). P values are for comparison between mock-infected mice and infected mice at the indicated time points. *, $P < 0.05$; **, $P < 0.01$; ***, $P < 0.001$; ND, not determined.

antibody response that is thought to be determinant for the protection (15, 21), we measured MAV-1-specific antibodies in the sera of infected mice at days 3, 7, 14, and 21 p.i. (Fig. 1d). We detected significant levels of MAV-1-specific antibodies from day 14 p.i. Furthermore, neutralizing antibody titers were quantified by neutralization assay (Fig. 1e). This analysis revealed the presence of neutralizing antibodies as early as day 7 p.i. and an increase of neutralizing antibody titers over all the subsequent time points that were tested. These results show that MAV-1 oral administration to mice results in a subclinical infection that allows generation of a specific and neutralizing humoral immune response against the virus similar to that generated by Ad4 and Ad7 vaccines in humans (15, 21).

MAV-1 oral immunization protects against a respiratory homologous challenge. Having established that oral infection with MAV-1 is nonpathogenic (based on a lack of clinical signs) and triggers an antiviral humoral immune response, we then wanted to know if this infection confers protection against intranasal challenge with the same virus, as is observed with human Ad4 and Ad7 vaccines (16). For this purpose, mice were immunized with 10^4 TCID₅₀ of MAV-1 or mock immunized orally. Then, at day 28 p.i., both mock- and MAV-1-treated groups were intranasally challenged or not with 10^5 TCID₅₀ of MAV-1 and euthanized at day 3, 7, 14, or 21 postchallenge (Fig. 2a). To evaluate the clinical condition of the mice, they were monitored and weighed from the day of oral immunization until the end of the experiment (Fig. 2b). Consistent with our previous results, MAV-1 oral infection did not induce any clinical signs or weight

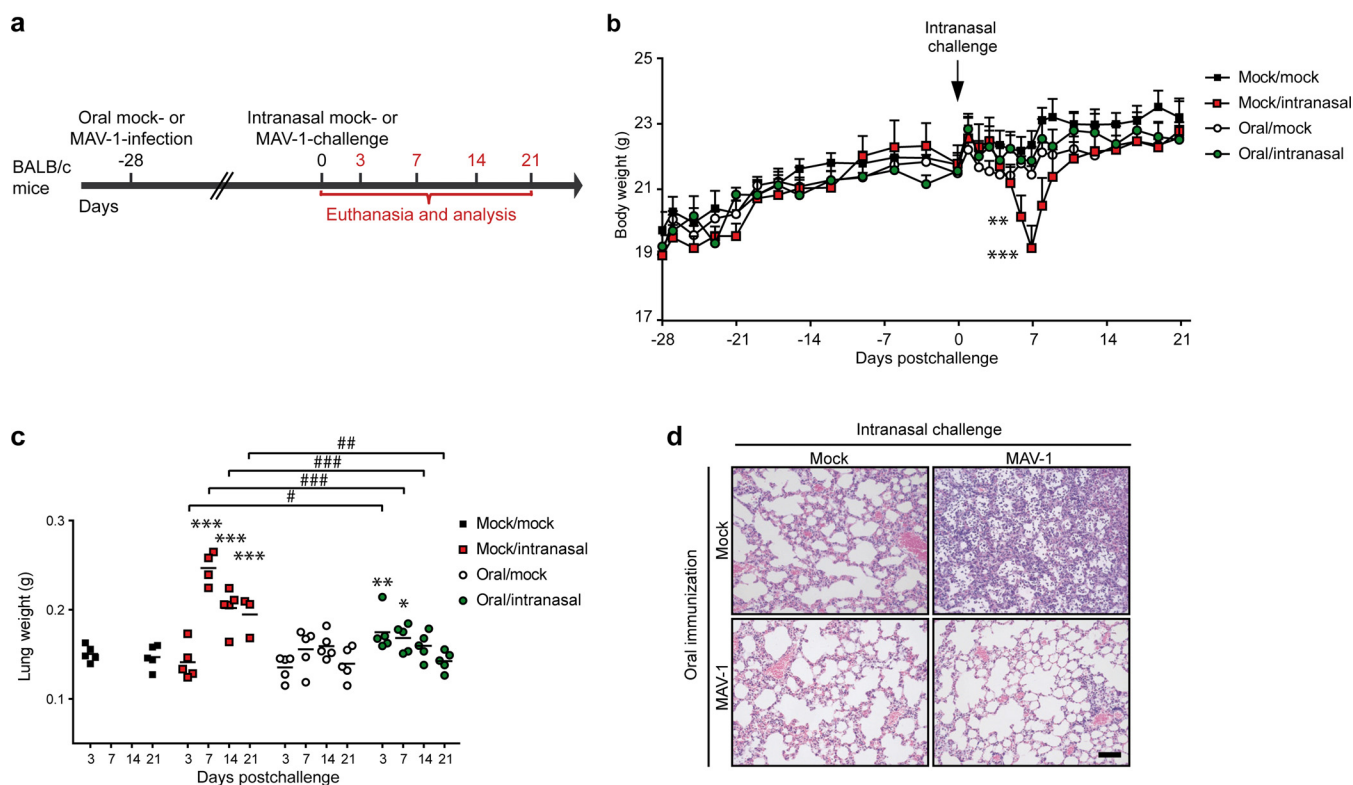


FIG 2 Evaluation of the protection induced by MAV-1 oral administration against a respiratory homologous challenge. (a) Eight-week-old female BALB/c mice were orally infected with 10^4 TCID₅₀ of MAV-1 or PBS as a control (mock). At 28 days p.i., the mice were challenged or not by intranasal administration of 10^5 TCID₅₀ of MAV-1 while they were under mild isoflurane anesthesia. Mice were euthanized at days 3, 7, 14, and 21 after intranasal challenge. Mice that did not receive MAV-1 either orally or intranasally (mock/mock) were euthanized at days 3 and 21 as negative controls ($n = 5$ in each group). (b) Weight of mice through day 21 postchallenge. For each time point, means were compared to the mean for the mock/mock group. (c) Weight of lungs at euthanasia. (d) Hematoxylin-eosin-stained sections of lungs at 7 days postchallenge. The images are representative of those from 3 animals. Bar, 100 μ m. Mock/mock (top left in panel d), mice that were not infected either orally or intranasally; mock/intranasal (top right in panel d), mice that were mock infected orally and then infected intranasally with MAV-1; oral/mock (bottom left in panel d), mice that were infected orally with MAV-1 and then mock infected intranasally; oral/intranasal (bottom right in panel d), mice that were infected orally with MAV-1 and then challenged intranasally with the same virus. The data presented are either the means for 5 mice \pm SEM (b) or individual data and means (c). Pooled data from naive mice at days 3 and 21 provided the negative control ($n = 10$). *P* values are for comparisons between the indicated time points (#, $P < 0.05$; ##, $P < 0.01$; ###, $P < 0.001$) or between mock-infected and the other groups of mice at the indicated time points (*, $P < 0.05$; **, $P < 0.01$; ***, $P < 0.001$).

loss until challenge. From 6 days postchallenge, nonimmunized intranasally challenged (mock/intranasal) mice began to develop clinical signs: all mice in this group experienced weight loss (on average, the loss of 14% of the initial mean weight), and some displayed a ruffled coat and/or a mild lethargy. These manifestations peaked at 7 days postchallenge, and then most mice recovered within 2 days. Two mice developed a more severe syndrome characterized by a hunched posture, ataxia, and lethargy and were euthanized at day 7 postchallenge ($>20\%$ weight loss). In contrast, mice that had previously been orally immunized (oral/intranasal) did not display any weight loss (Fig. 2b) or clinical signs after the intranasal challenge.

MAV-1 intranasal infection of mice generates an inflammatory response in lungs that is histologically characterized by a substantial cellular infiltrate in peribronchiolar regions (30, 32). In order to compare pulmonary inflammation in the different groups, lungs were isolated and weighed after MAV-1 intranasal challenge (Fig. 2c). While there was no difference between the lungs from mock-immunized, mock-infected (mock/mock) mice and those from orally immunized, mock-infected (oral/mock) mice, the lungs from mock/intranasal mice were significantly heavier at days 7, 14, and 21 postchallenge (Fig. 2c). The lung weights of mice orally immunized before intranasal challenge (oral/intranasal) were higher than those of mock/mock mice only at days 3 and 7 postchallenge. Moreover, after challenge, comparison between the mock/intranasal and oral/intranasal groups highlighted differences at all time points tested.

Indeed, while at day 3 after intranasal challenge lung weights were higher in oral/intranasal mice, the opposite was observed at days 7, 14, and 21 postchallenge. These data suggest that MAV-1 oral immunization led to an immediate and moderate inflammatory reaction in the lungs at day 3 postchallenge and subsequently reduced the inflammation induced by the intranasal homologous challenge.

These observations were confirmed by histological analyses on lung samples at day 7 postchallenge (Fig. 2d). Thus, the lungs from oral/mock mice were apparently devoid of inflammation and similar to those from mock/mock mice. Consistent with previous studies (30, 32), the lungs from mock/intranasal mice displayed a massive infiltration of inflammatory cells, essentially localized in the lumen of the alveoli. In contrast, in oral/intranasal mice, there was no prominent infiltration, and the general appearance was comparable to that of the lungs from mock/mock mice. Altogether, these results show that MAV-1 oral immunization protects from the severe clinical signs and massive lung inflammation that are observed following a respiratory infection with MAV-1.

MAV-1 oral immunization triggers B and CD8 T cell responses. We then characterized the pulmonary immune cell infiltration in these 4 groups at day 7 postchallenge (Fig. 3a). In mock/intranasal mice, we observed a massive cellular infiltrate composed of neutrophils, inflammatory monocytes (Ly6C^{hi} monocytes), and NK cells both in bronchoalveolar lavage (BAL) fluid (BALF) (Fig. 3b) and in the lung parenchyma (Fig. 3c). In contrast, this infiltration of innate immune cells was nearly totally abolished in oral/intranasal mice (Fig. 3b and c). In those mice, we observed the tissue infiltration of CD8 T cells that displayed mainly an effector memory phenotype (CD62L[−] CD44^{hi}) (Fig. 3c) and the presence of a significant amount of B cells in the airways (Fig. 3b). This suggests that oral immunization with MAV-1 triggers the development of an adaptive immune response that contributes to protection against a subsequent respiratory challenge with the same virus.

MAV-1 oral immunization reduces viral replication after a respiratory homologous challenge but leads to a systemic infection. We then compared the viral loads of MAV-1 in the lungs after intranasal infection of mice that had previously been orally immunized or not (Fig. 4a). We assessed the presence of the virus by qPCR (Fig. 4b). As expected, the level of viral DNA detected in lungs from mock/intranasal mice was higher at days 3, 7, and 14 postchallenge than in lungs from oral/intranasal mice. These results indicate that MAV-1 oral immunization at least partially protects against viral infection in the lungs during intranasal challenge. Surprisingly, we also detected viral DNA in the oral/mock group, suggesting that the virus spread to the lungs after oral administration.

To investigate the potential systemic dissemination of the virus, we evaluated the presence of the virus in blood and in various organs at different time points after oral immunization (Fig. 4c to e). In blood, viral DNA was detected as early as 3 days p.i. in some mice and was still detected in some mice at 21 days p.i. (Fig. 4d). To localize the sites of infection in the digestive tract, we dissected the gut into duodenum, jejunum, and ileum and isolated Peyer's patches from these respective parts. MAV-1 genomes were detected in all segments of the small intestine and in all corresponding Peyer's patches at day 7 p.i. High levels of viral genomes were also detected in Peyer's patches of the duodenum at days 14 and 21 p.i. (Fig. 4e). In contrast, MAV-1 genomes were only sporadically detected in the jejunum and ileum and in the corresponding Peyer's patches at days 14 and 21 p.i. We then assessed the presence of the virus in draining mesenteric lymph nodes and spleen. Significant levels of viral DNA were detected at all time points tested from day 7 p.i. Viral DNA was also detected in liver, lungs, heart, and brain from infected mice (Fig. 4e). The highest levels of viral genomes were detected at day 7 p.i. in liver and lungs and at day 14 p.i. in heart and brain (Fig. 4e). Previous studies have reported infection of these organs after MAV-1 intraperitoneal or intranasal administration (35–37) as well. These results indicate that MAV-1 orally administered to mice leads not only to infection of the small intestine and Peyer's patches but also to its systemic dissemination throughout the body.



We next tested whether oral administration of a lower dose of MAV-1 could confer protection while avoiding the systemic infection observed with 10^4 TCID₅₀. We immunized mice with 1, 10, 10^2 , 10^3 , or 10^4 TCID₅₀. At day 28 p.i., mice were intranasally challenged with 10^5 TCID₅₀ as described above (Fig. 5a). Daily weighing up to 14 days postchallenge showed that mice orally immunized with 10^2 TCID₅₀ or more did not display any notable weight loss, suggesting that these mice might have been effectively protected (Fig. 5b). These results were confirmed by serological analyses for mice immunized with 10^2 TCID₅₀ or more, since we detected a MAV-1-specific and -neutralizing antibody response (Fig. 5c and d). Based on these results, we infected mice orally with 10^2 TCID₅₀ to determine whether this lower protective dose also induced a systemic infection (Fig. 6a). The qPCR analyses performed on the digestive tract (duodenum, jejunum, ileum, and their respective Peyer's patches), lymphoid organs (mesenteric lymph nodes, and spleen), and distal organs (lungs and brain) showed the presence of viral DNA in all these tissues in amounts similar to those detected after oral administration of 10^4 TCID₅₀ of MAV-1 (Fig. 6b). The only obvious difference between the qPCR results obtained after a high dose (Fig. 4) and a low dose (Fig. 6) was the kinetics of infection. After oral infection with the lower dose, the peak of viral DNA was delayed from day 7 to day 14 p.i. in most of the analyzed organs. These results show that oral administration of 10^2 TCID₅₀ was sufficient to induce a specific and neutralizing humoral response against MAV-1 and to prevent the weight loss associated with an intranasal challenge. However, this lower dose was also associated with a systemic infection.

Oral immunization with a live vaccine better protects than intramuscular immunization with an inactivated vaccine against a respiratory MAV-1 homologous challenge. Because systemic dissemination of the live adenovirus vectors is potentially harmful, we then determined if live oral vaccine offers advantages, other than the practical route of administration benefit, compared to an alternative inactivated intramuscular immunization (Fig. 7 to 9). We immunized mice orally or intramuscularly either with 10^4 TCID₅₀ of live MAV-1 or with the same dose of formalin-inactivated virus. Twenty-eight days later, the mice were challenged intranasally with the same virus and euthanized for analysis at day 7 postchallenge (Fig. 7a). As previously observed, mice orally immunized with the live vaccine (oral live/intranasal) were completely protected against weight loss. Similarly, mice immunized intramuscularly with the live vaccine (intramuscular live/intranasal) or inactivated vaccine (intramuscular inactivated/intranasal) were also protected (Fig. 7b). Mice orally immunized with the inactivated virus (oral inactivated/intranasal) displayed a limited weight loss compared to the nonimmunized control mice (Fig. 7b). Next, we evaluated the viral loads in the lungs at day 7 postchallenge. This revealed a decrease in the number of viral genomes detected in mice immunized with live vaccines intramuscularly or orally and, to a lesser extent, in mice immunized intramuscularly with the inactivated vaccine. Mice immunized orally with the inactivated vaccine did not display any reduction in the number of viral genomes in the lungs (Fig. 7c). We then assessed the presence of MAV-1-specific total Ig and IgA in serum and BALF at day 7 postchallenge (Fig. 7d). We found specific antibodies in serum and BALF in all immunized mice except those immunized orally with the inactivated vaccine. While no specific IgA was detected in serum, specific IgA was present in the BALF from the groups of mice immunized orally with the live vaccine or intramuscularly with the live or inactivated vaccine, with the highest levels being observed in the last two groups (Fig. 7d). The neutralization capacity of the serum correlated with the amount of

FIG 3 Characterization of lung immune cell populations after MAV-1 oral immunization and challenge. (a) Eight-week-old female BALB/c mice ($n = 5$ per group) were orally infected with 10^4 TCID₅₀ of MAV-1 or PBS as a control (mock). At 28 days p.i., mice were challenged by intranasal administration of 10^5 TCID₅₀ of MAV-1 while they were under mild isoflurane anesthesia. Mice were euthanized at day 7 after intranasal challenge. (b) Gating strategy (top) and total numbers (bottom) of immune cell populations in BALF. (c) Gating strategy (top) and total numbers (bottom) of immune cell populations in lungs. P values are for comparisons between all pairs of groups. *, $P < 0.05$; **, $P < 0.01$; ***, $P < 0.001$. SSC, side scatter; FSC, forward scatter; AM, alveolar macrophages; Neutro, neutrophils; MO, monocytes; Leu, leukocytes; Eosino, eosinophils; T_{EM} cells, effector memory T cells.

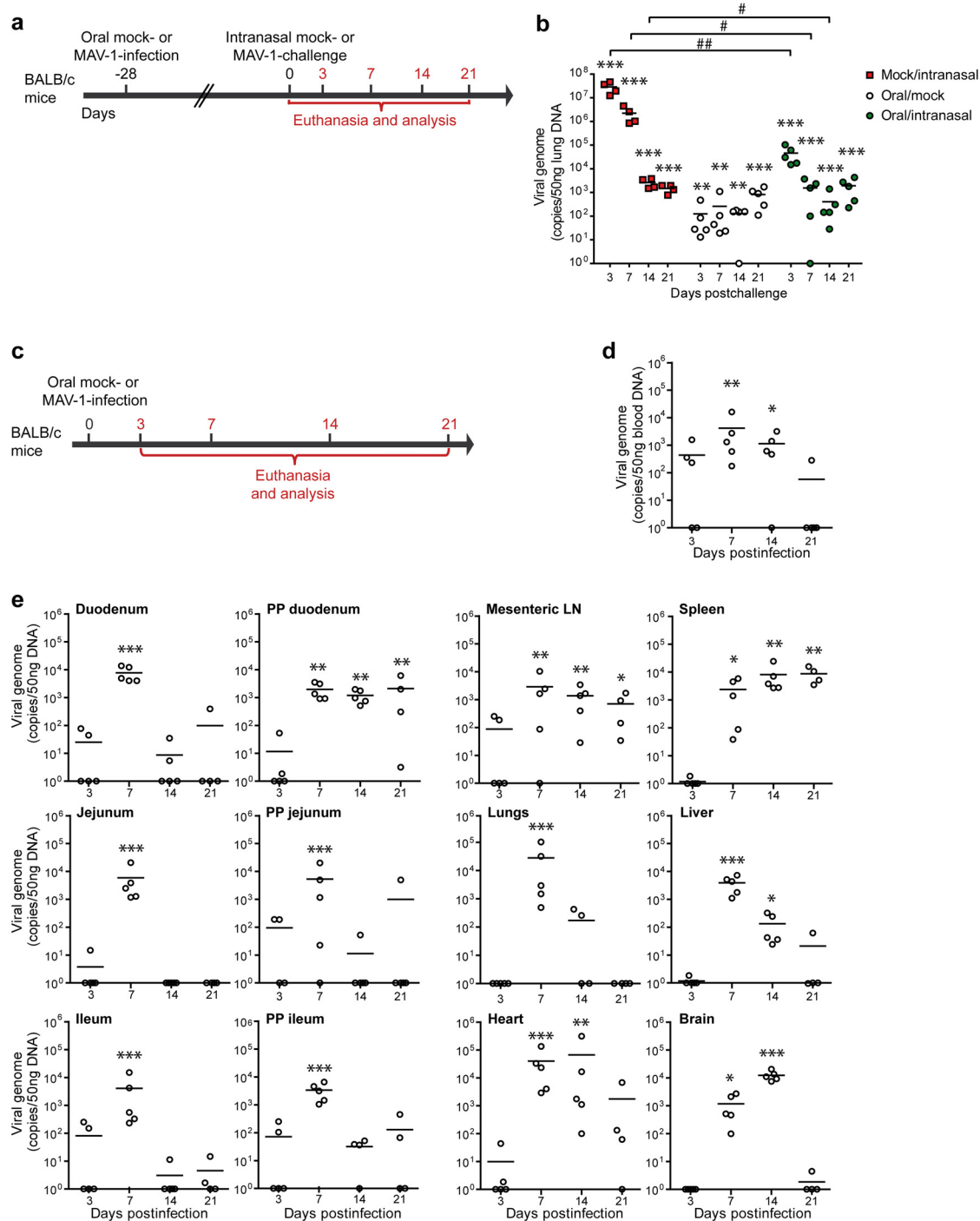


FIG 4 MAV-1 distribution after oral immunization and challenge. (a) Eight-week-old female BALB/c mice ($n = 5$ per group) were orally infected with 10^4 TCID₅₀ of MAV-1 or PBS as a control (mock). At 28 days p.i., mice were challenged by intranasal administration of 10^5 TCID₅₀ of MAV-1 while they were under mild isoflurane anesthesia. Mice were euthanized at day 7 after intranasal challenge. (b) MAV-1 genome copy numbers in lungs. (c) Eight-week-old female BALB/c mice were orally infected with 10^4 TCID₅₀ of MAV-1 or PBS (mock) and euthanized at days 3, 7, 14, or 21 p.i. for analysis ($n = 5$ in each group). The numbers above the arrow indicate the day p.i. (d) MAV-1 genome copy numbers in blood. (e) MAV-1 genome copy numbers in organs. PP, Peyer's patches; LN, lymph nodes. The data presented are individual data and means. Pooled data from naive mice at days 3 and 21 provided the negative control ($n = 10$). P values are for comparisons between the indicated time points (#, $P < 0.05$; ##, $P < 0.01$) or between the mock-infected group and the other groups at the indicated time points (*, $P < 0.05$; **, $P < 0.01$; ***, $P < 0.001$).

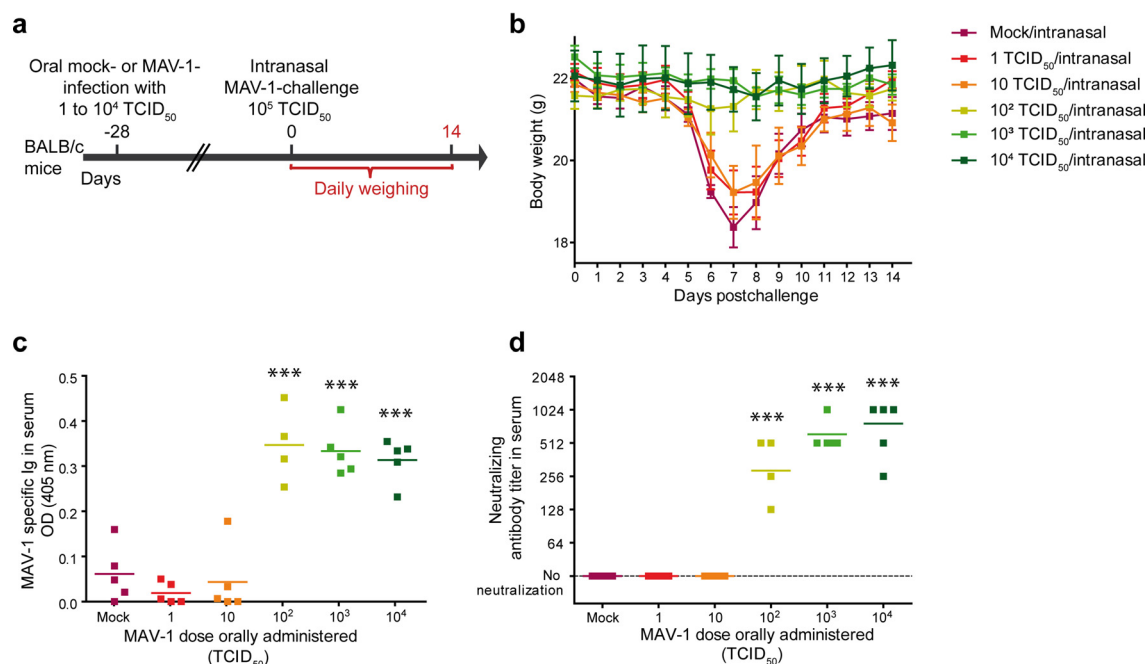


FIG 5 Comparison of the protection induced by different doses of MAV-1 against a respiratory homologous MAV-1 challenge. (a) Eight-week-old female BALB/c mice ($n = 5$ per group) were orally infected with 1, 10, 10^2 , 10^3 , or 10^4 TCID₅₀ of MAV-1 or PBS as a control (mock). At 28 days p.i., mice were challenged by intranasal administration of 10^5 TCID₅₀ of MAV-1 while they were under mild isoflurane anesthesia. Mice were euthanized at day 14 after intranasal challenge. (b) Weight of mice from day 0 to day 14 postchallenge. The data presented are the average for 5 mice \pm SEM. For each time point, means were compared to the mean for mice in the mock/intranasal group. Statistically significant differences were observed between mice challenged with 10^2 , 10^3 , and 10^4 TCID₅₀ and the mock/intranasal group at days 6, 7, 8, and 9 p.i.; for clarity, this is not represented on the graph. (c and d) MAV-1-specific antibodies (c) and MAV-1-neutralizing antibody titers (d) after oral immunization but before challenge (day 0). OD, optical density. Individual data are presented, and means are shown by a line. P values are for comparison between mock-infected mice and mice receiving the indicated MAV-1 doses. ***, $P < 0.001$.

specific total Ig (Fig. 7e). In the BALF, complete neutralization (used to determine the neutralizing antibody titer) was achieved only in the groups immunized with the live vaccines (Fig. 7e).

We then characterized the immune cell populations in BALF and lungs by flow cytometry analysis at 7 days postchallenge (Fig. 8 and 9). Live vaccines administered orally or intramuscularly almost completely protected against neutrophil, NK cell, and inflammatory monocyte infiltration in the BALF and in the lung parenchyma (Fig. 8b and c and Fig. 9b and c). In comparison, the inactivated intramuscular vaccine conferred only partial protection against inflammatory cell infiltration. In the groups of mice immunized orally with inactivated MAV-1, although we did not observe any protection in the lungs (Fig. 8c and 9c), we detected a decrease in the number of NK cells and inflammatory monocytes in BALF (Fig. 8b and 9b). In contrast, the numbers of B cells and CD4, CD8, and effector memory (CD62L[−] CD44^{hi}) CD8 T cells were markedly higher in the lungs of mice immunized intramuscularly with live MAV-1 than in the lungs of mice in the other groups. The number of these adaptive immune cells was similar in mice intramuscularly immunized with the inactivated MAV-1 and mice orally immunized with the live vaccine, except for effector memory CD8 T cells, which were more numerous in the latter group (Fig. 8c and 9c). Altogether, these results show that although the intramuscular immunization of live MAV-1 conferred a better adaptive immune response than the oral immunization of live MAV-1, these two vaccines protected similarly against weight loss, viral replication, and lung inflammation. In contrast, the intramuscular inactivated vaccine only partially prevented pulmonary inflammation and conferred a weaker protection against viral lung infection, despite eliciting higher levels of anti-MAV-1 IgA in BALF.

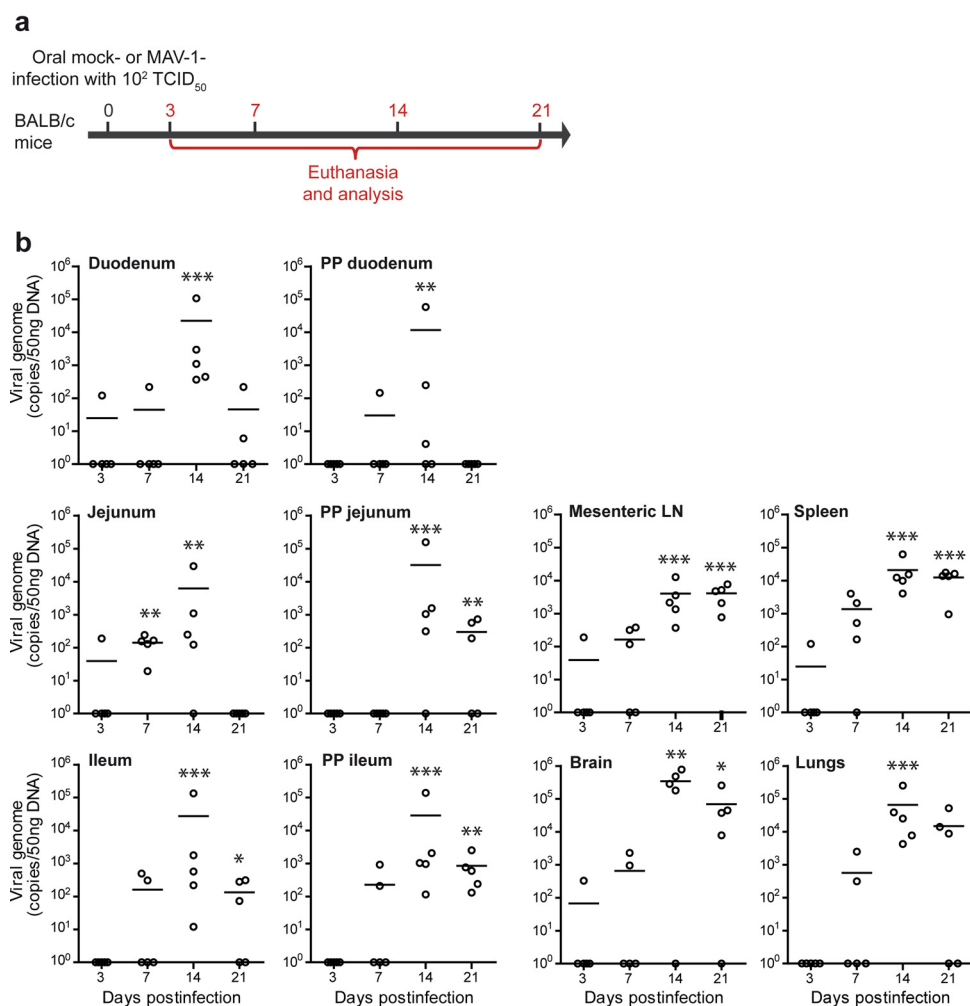


FIG 6 Dissemination of MAV-1 in BALB/c mice after a low-dose oral infection. (a) Eight-week-old female BALB/c mice were orally infected with 10^2 TCID₅₀ of MAV-1 or PBS (mock) and euthanized at day 3, 7, 14, or 21 p.i. for analysis ($n = 5$ mice in each group). The numbers above the arrow indicate the day postinfection. (b) MAV-1 genome copy numbers in organs. Individual data and means are presented. Pooled data from naive mice at days 3 and 21 provided the negative control ($n = 10$). P values are for comparison between the mock-infected group and the other groups of mice at the indicated time points. *, $P < 0.05$; **, $P < 0.01$; ***, $P < 0.001$. PP, Peyer's patches; LN, lymph nodes.

DISCUSSION

Oral administration of replication-competent adenovirus-vectored vaccines is a promising approach for mass vaccination in either animal or human populations. In particular, attention has been paid to the development of oral replication-competent vectors based on human Ad4 and Ad7, because these viruses have been used since the 1970s as oral live vaccines in U.S. military forces (13–17). Usage of these vaccines may need to be increased in the coming years, since recent studies reported an apparent increase in the frequency of human Ad4 infections among general populations in the past 10 years (38, 39). This observation could be linked to the evolution of the virus. Indeed, while Ad4 was one of the first viral respiratory pathogens to be isolated (40), the fact that it likely originates from chimpanzees was only recently described (41, 42). The genomes of simian adenoviruses and the prototype Ad4 do not contain specific replication motifs in their inverted terminal repeats (such as the human NF-I transcription factor binding site), therefore limiting the circulation of these viruses in human populations. However, most emergent Ad4 isolates have this NF-I binding site, suggesting that the occurrence of Ad4-related diseases could increase in the future. Similarly, human adenoviruses species B, such as Ad7, also likely originated from African

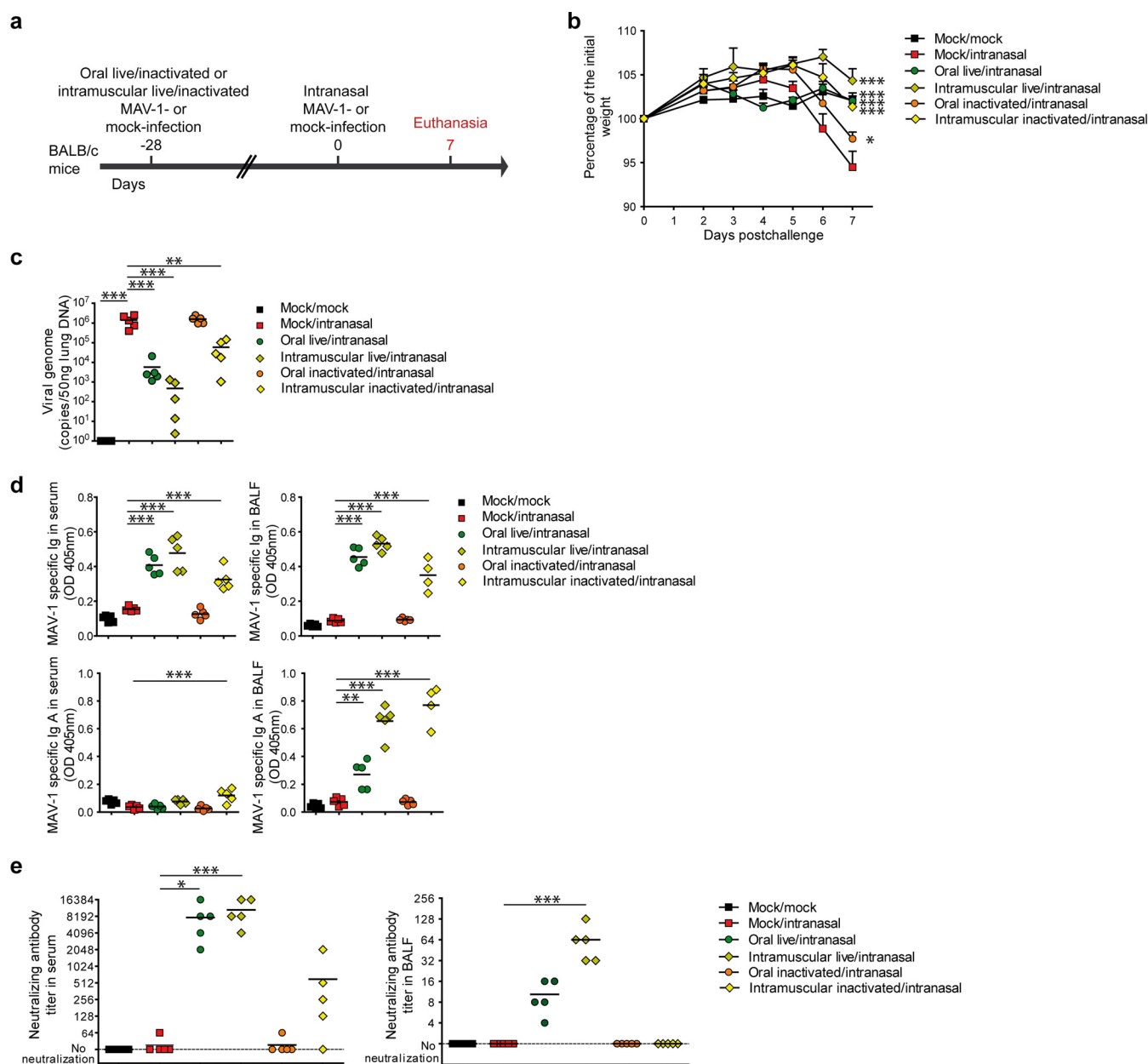


FIG 7 Comparison of the protection induced by live or inactivated MAV-1 oral or intramuscular immunization against a respiratory homologous challenge. (a) Eight-week-old female BALB/c mice ($n = 5$ per group) were orally or intramuscularly immunized with 10^4 TCID₅₀ of live MAV-1 or the same dose of formalin-inactivated MAV-1. At 28 days p.i., mice were challenged by intranasal administration of 10^5 TCID₅₀ of live MAV-1 while they were under mild isoflurane anesthesia. Mice were euthanized at day 7 postchallenge. (b) Weight of mice after challenge. (c) MAV-1 genome copy numbers in lungs at day 7 postchallenge. (d) MAV-1-specific total immunoglobulin (Ig) and IgA in serum and BALF at day 7 postchallenge. (e) MAV-1-neutralizing antibodies in serum and BALF at day 7 postchallenge. Mock/mock, mice that were not infected either orally or intranasally; mock/intranasal, mice that were mock infected orally and then infected intranasally with live MAV-1; oral live/intranasal, mice that were infected orally with live MAV-1 and then challenged intranasally; intramuscular live/intranasal, mice that were infected intramuscularly with live MAV-1 and then challenged intranasally; oral inactivated/intranasal, mice that were infected orally with inactivated MAV-1 and then challenged intranasally; intramuscular inactivated/intranasal, mice that were infected intramuscularly with inactivated MAV-1 and then challenged intranasally. The data presented are either the means for 5 mice \pm SEM (b) or individual data and means (c, d, e). *P* values are for comparison between all pairs of groups. For clarity, only differences between the mock/intranasal and the other groups are shown and only differences for day 7 postchallenge are shown in the weight curve. *, $P < 0.05$; **, $P < 0.01$; ***, $P < 0.001$.

great apes and may also pose new global challenges for human health, as recently observed (43). A better knowledge of replication-competent oral adenovirus vaccines is therefore of major importance.

Until now, the development of such vaccines has been hampered by the lack of any reliable small-animal model. In this study, we characterized MAV-1 oral infection of

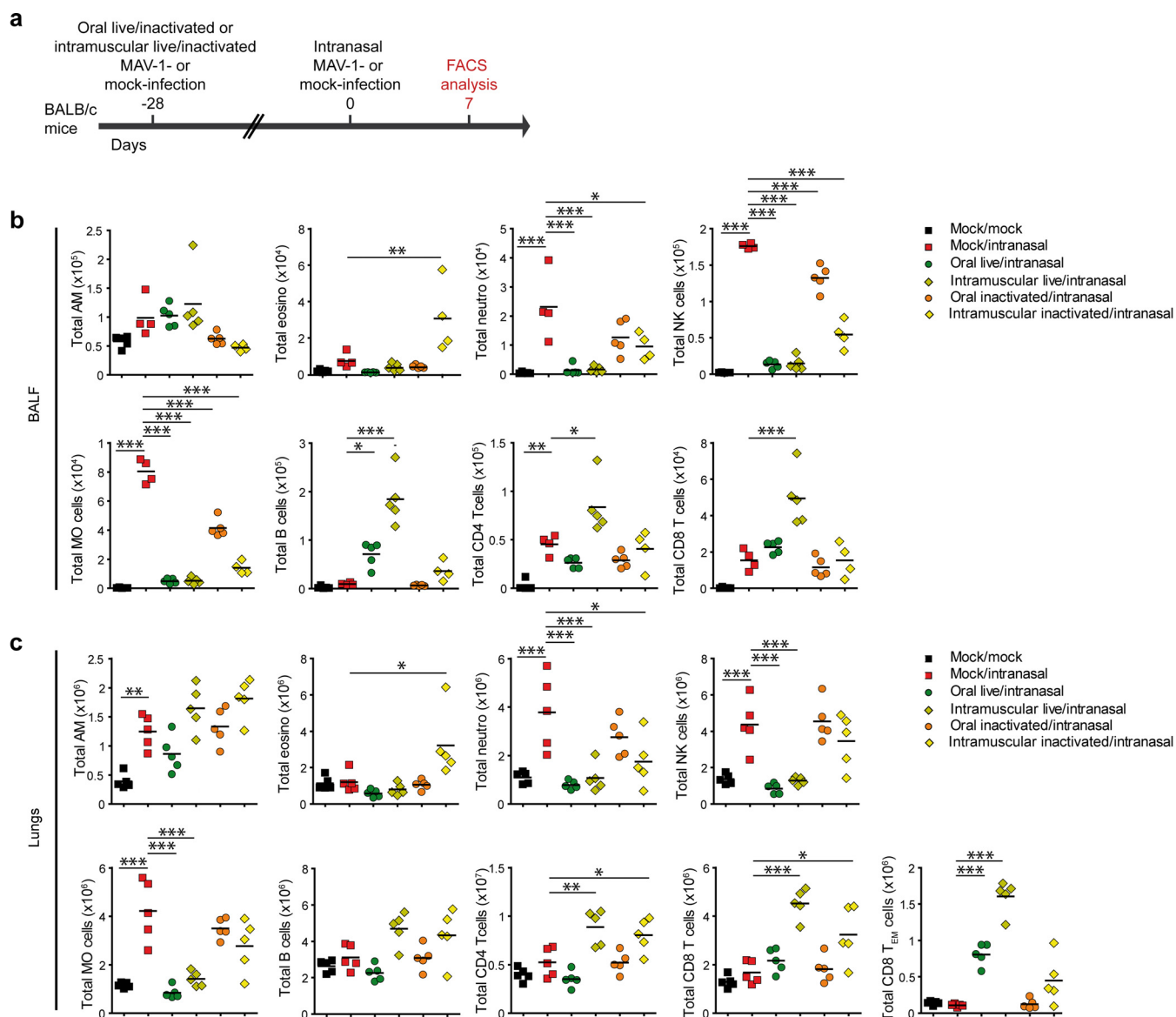


FIG 8 Characterization of lung immune cell populations after live or inactivated MAV-1 oral or intramuscular immunization and challenge. (a) Eight-week-old female BALB/c mice ($n = 5$ per group) were orally or intramuscularly infected with 10^4 TCID₅₀ of live MAV-1 or the same dose of formalin-inactivated MAV-1. At 28 days p.i., mice were challenged by intranasal administration of 10^5 TCID₅₀ of live MAV-1 while they were under mild isoflurane anesthesia. Mice were euthanized at day 7 postchallenge. (b) Total numbers of immune cell populations in BALF. (c) Total numbers of immune cell populations in lung parenchyma. Mock/mock, mice that were not infected either orally or intranasally; mock/intranasal, mice that were mock infected orally and then infected intranasally with live MAV-1; oral live/intranasal, mice that were infected orally with live MAV-1 and then challenged intranasally; intramuscular live/intranasal, mice that were infected intramuscularly with live MAV-1 and then challenged intranasally; oral inactivated/intranasal, mice that were infected orally with inactivated MAV-1 and then challenged intranasally; intramuscular inactivated/intranasal, mice that were infected intramuscularly with inactivated MAV-1 and then challenged intranasally. The data presented are individual data and means. P values are for comparison between all pairs of groups. For clarity, only differences between the mock/intranasal and the other groups are shown. *, $P < 0.05$; **, $P < 0.01$; ***, $P < 0.001$. AM, alveolar macrophages; neutro, neutrophils; MO, monocytes; eosino, eosinophils; T_{EM} cells, effector memory T cells.

BALB/c mice as a mouse model for Ad4- and Ad7-based vaccines. First, we showed that MAV-1 oral infection does not induce any clinical signs in BALB/c mice. Second, we showed that MAV-1 oral immunization protects mice against a respiratory challenge with the same virus. Third, we showed that MAV-1 oral infection spreads systemically, as demonstrated by the detection of viral DNA in multiple organs. Finally, we compared the immune responses induced by the live vaccine given orally or intramuscularly and those induced by formalin-inactivated vaccines.

Oral administration of MAV-1 did not induce any weight loss (Fig. 1) but triggered the development of a specific adaptive immune response that protected the mice



against respiratory homologous challenge (Fig. 2), thus reproducing in mice what it is observed with human Ad4 and Ad7 vaccines (21). Ad4 and Ad7 vaccines are thought to cause a transient subclinical infection of the gut and not disseminate beyond the intestinal tract and especially not disseminate to the blood, urine, or throat (15, 21). In contrast, our results showed that after initial replication in the small intestine, MAV-1 disseminated all over the body (Fig. 4). Indeed, after oral immunization, we observed a peak of viral DNA at 7 days p.i. in all segments of the intestine tested, suggesting that the virus not only enters the body through the gut but also replicates at that site. This observation parallels the findings of studies on Ad4 and Ad7 vaccines that identified the presence of virus in the stools of vaccinated people up to 28 days p.i. (15). The same study also reported that the virus shedding in feces was observed only sporadically and not in all vaccine recipients (15). These data are consistent with those from our murine model, in which we found viral DNA in feces from infected mice only sporadically (Fig. 1c). For human Ad4 and Ad7 vaccines, the specific sites of infection in the gut are not known (21). Human Ad5 targets M cells in a Caco-2 cell model of intestinal epithelium (44). We thus investigated the presence of the virus in Peyer's patches of each segment of the gut and found viral genomes in Peyer's patches from all of them. While the levels of viral genomes peaked at day 7 p.i. and then decreased in Peyer's patches from the jejunum and the ileum, viral levels stayed high up to day 21 p.i. in Peyer's patches from the duodenum, suggesting a preferential site of replication (Fig. 1c). Despite the detection of viral genomes, histological analyses did not reveal any obvious differences between Peyer's patches from uninfected and infected mice (data not shown). To precisely locate the sites of infection and the targeted cells in the future, identification of viral antigens in specific cell subsets will be useful.

Unexpectedly, besides the digestive tract, MAV-1 was also detected in the mesenteric lymph nodes, spleen, and all the distal organs that we tested (Fig. 4). These observations were made with a dose as low as 100 TCID₅₀ of MAV-1 administered orally (Fig. 6). These results may portend a similar biodistribution for Ad4 and Ad7 in humans. The human Ad4 and Ad7 vaccines contain at least 3.2×10^4 TCID₅₀ of Ad4 and Ad7. While Ad4 and Ad7 oral vaccines have acceptable safety profiles, as demonstrated over many years in thousands of recipients, the knowledge acquired on these vaccines is based on their use in only a very specific population. Ad4 and Ad7 vaccines are exclusively approved for use by U.S. military forces and are essentially administered to new military recruits, i.e., young people in good health. A broader use of these viruses as vaccine platforms in a large population must therefore be considered with caution, considering the potential dissemination of the virus throughout the body. In addition, the understanding of the events that occur following the release of Ad4 and Ad7 vaccines in the gut is very limited. To date, the data consist of clinical observations, serology, and screening for virus in blood, stool, rectal swabs, and throat swabs at only a few time points after vaccine administration. In particular, the absence of viremia was diagnosed only based on analysis of blood collected and frozen at days 0, 7, 28, and 56 after vaccination and then cultured in order to reveal the presence of adenoviruses (15). It is thus possible that viremia occurs at time points that have not been tested. Additionally, it is possible that the adenovirus culture approach was not sensitive enough to detect virus in blood, as suggested by the negative results obtained by blood culture for two vaccine placebo recipients who developed an Ad4 infection

FIG 9 Gating strategy used for the characterization of lung immune cell populations of MAV-1-challenged mice after different immunization protocols (a) Eight-week-old female BALB/c mice ($n = 5$ per group) were orally or intramuscularly infected with 10^4 TCID₅₀ of live MAV-1 or the same dose of formalin-inactivated MAV-1. At 28 days p.i., mice were challenged by intranasal administration of 10^5 TCID₅₀ of live MAV-1 while they were under mild isoflurane anesthesia. Mice were euthanized at day 7 postchallenge. (b) Representative dot plots in BALF. (c) Representative dot plots in lung parenchyma. Mock/i.n., mice that were mock infected orally and then infected intranasally with live MAV-1; oral live/i.n., mice that were infected orally with live MAV-1 and then challenged intranasally; i.m. live/i.n., mice that were infected intramuscularly with live MAV-1 and then challenged intranasally; oral inact./i.n., mice that were infected orally with inactivated MAV-1 and then challenged intranasally; i.m. inactivat./i.n., mice that were infected intramuscularly with inactivated MAV-1 and then challenged intranasally; AM, alveolar macrophages; Neutro, neutrophils; MO, monocytes; Leuco, leucocytes; Eosino, eosinophils; T_{EM} cells, effector memory T cells.

during the trial, while they were positive by qPCR of throat swab samples (15). However, this discrepancy could be inherent to the two techniques, with qPCR measuring the viral DNA and blood culture quantifying infectious particles. In that context, it will be important to compare the qPCR and culture methods for various tissues in our MAV-1 model, in order to further evaluate the sensitivity of these approaches and to characterize the kinetics of the viremia following oral administration.

Besides viral dissemination, the study of MAV-1 oral inoculation of mice also sheds new light on the possible mechanisms involved in the protection conferred by Ad4 and Ad7 vaccines against a respiratory homologous challenge. In humans, those vaccines are thought to mediate protection by inducing a protective antibody response (15, 21). However, the mechanism of action of Ad4 and Ad7 vaccines has never been addressed directly, and besides antibody, cells such as CD8 T cells could also play a role. Similar to what is observed for Ad4 and Ad7, oral administration of MAV-1 induced a strong protective antibody response that could be found in both serum and BALF after respiratory challenge (Fig. 1 and 7). Surprisingly, after respiratory homologous challenge, we observed less IgA in the BALF of mice that received the live oral vaccine than in mice that received the live or inactivated vaccine intramuscularly (Fig. 7d). In the case of influenza virus infection in mice (45), IgA mediates protection of the upper respiratory tract, while IgG protects the lungs. The fact that mice that received the live MAV-1 oral vaccine did not develop a strong IgA response in BALF but displayed high levels of total immunoglobulins is therefore probably not a weakness for the protection against pneumonia. Besides antibodies, we also showed that mice that received the oral live vaccine displayed a good effector CD8 T cell response after challenge, suggesting that those cells could also play a role in the protection against MAV-1 respiratory challenge. Our results therefore suggest that, as previously thought, oral live Ad4 and Ad7 vaccines probably protect against a respiratory challenge by inducing a strong neutralizing antibody response. However, the important Ig isotype is probably not IgA, because mice that received the intramuscular inactivated vaccine were not fully protected, despite displaying the highest level of specific IgA in BALF (Fig. 5d). Moreover, the presence in lung parenchyma of effector CD8 T cells in all groups that were protected against the respiratory challenge (Fig. 6d) suggests that those cells probably play a major role in protection.

Altogether, we have demonstrated that oral administration of MAV-1 protects mice against a homologous respiratory challenge, establishing a reliable model for oral vaccination based on replication-competent adenoviruses, such as human Ad4 and Ad7 vaccines. However, it must be emphasized that our results have also highlighted a potential risk of systemic infection by replication-competent adenoviruses administered orally. These results therefore suggest that we should use the utmost caution in evaluating the safety of potential oral replication-competent adenovirus-based vectors.

MATERIALS AND METHODS

Animals. All animal work complied with relevant European, federal, and institutional policies. The Committee on the Ethics of Animal Experiments of the University of Liège reviewed and approved the protocol (permit number 1526). Female BALB/c mice were purchased from Envigo. All mice were housed in the University of Liège Department of Infectious Diseases. The animals were infected orally or intranasally with MAV-1 when they were 7 to 8 and 11 to 13 weeks old, respectively. For oral infections, 10^4 TCID₅₀ (or the dose indicated elsewhere in the article) of MAV-1 diluted in 250 μ l of phosphate-buffered saline (PBS) was administered into the esophagus with a steel feeding gavage needle. For intramuscular immunization, 10^4 TCID₅₀ (or the dose indicated elsewhere in the article) of MAV-1 (inactivated or not) diluted in 30 μ l of PBS was administered into one gastrocnemius with an insulin syringe. For intranasal infections, 10^5 TCID₅₀ of MAV-1 diluted in 30 μ l of PBS was inoculated while the mice were under mild isoflurane anesthesia. To evaluate clinical signs of infection, we monitored and weighed the mice daily for 8 days p.i. and then every other day. Ruffled coat, loss of activity, and weight loss below 20% were considered signs of moderate pain and distress; hunched posture, ataxia, lethargy, and weight loss greater than 20% were considered signs of severe pain and distress and constituted endpoint criteria.

Virus and cells. We used the pmE101 wild-type strain of MAV-1 for this work (46, 47). The virus was grown on mouse 3T6 cells cultivated in Dulbecco's modified Eagle's medium (DMEM; Life Technologies) supplemented with 2 mM glutamine, 100 U penicillin ml⁻¹, 100 mg streptomycin ml⁻¹, and 5% heat-inactivated fetal calf serum (FCS) in an atmosphere of 5% CO₂. The particle-to-number-of-PFU ratio was

estimated based on the number of MAV-1 genomes per TCID₅₀ (measured by quantitative PCR and titration, respectively). This ratio was about 10⁴ for each viral stock that we used.

Virus titration. For titration, subconfluent 3T6 cells in 96-well plates were infected with 10-fold serial dilutions (from 10⁻¹ to 10⁻⁸) of the viral samples in DMEM supplemented as described above; 10 replicates were made for each dilution. After 14 days, cells were fixed in 2% paraformaldehyde for 20 min at room temperature (RT) and then washed 2 times in PBS and blocked for 30 min with PBS, 10% FCS, 300 mM glycine. Cells were then incubated at 4°C for 2 h with a primary rabbit polyclonal antiserum directed against MAV-1 purified virions (AKO-1-68) (48) diluted 1,000-fold in the blocking solution. Cells were washed 3 times in PBS and then incubated at RT for 30 min with a goat anti-rabbit IgG secondary antibody conjugated with Alexa Fluor 488 (1 µg/ml; Life Technologies). After 3 washes in PBS, the cells were observed and the titer (number of TCID₅₀ per milliliter) of viral production was determined using the classical Reed and Muench method (49). For inactivation, the virus was incubated for 72 h at 37°C in 0.025% formol and then dialyzed in Slide-A-Lyzer dialysis cassettes (molecular weight cutoff, 20 kDa; Thermo Fisher) in PBS 2 times for 2 h each time and once overnight at 4°C.

In vivo sample collection and processing. Mice were euthanized by isoflurane inhalation, and then their blood, organs, and feces were collected. For viral titration and for qPCR analyses, whole organs were harvested and kept on ice during dissection. Each organ was disrupted in 1 ml PBS using TissueLyser II solution (Qiagen) and either directly used for analyses or stored at -20°C until further processing. For histological analyses, lungs were harvested and fixed in 10% formalin. After 24 h in formalin, the tissues were transferred to 70% ethanol until they were embedded in paraffin.

Viral genome quantification. DNA was extracted from disrupted organs with a Wizard genomic DNA purification kit (Promega). Viral genome loads were measured by real-time PCR. Briefly, 50 ng of extracted DNA was added to a reaction mixture containing TaqMan Universal PCR mix (Life Technologies), forward and reverse primers (each at a 400 nM final concentration), and probe (final concentration, 200 nM) in a total volume of 25 µl. Primers were chosen to amplify a 167-bp fragment within the MAV-1 hexon DNA sequence (forward primer, 5'-GGCCAACACTACCGACACTT-3'; reverse primer, 5'-TTTTGTCTGTGGCATTGA-3'), and these PCR products were quantified by hybridization with a TaqMan probe (5'-FAM-CATTCCAGCCAATTATGGCTCGGC-TAMRA-3', where FAM is 6-carboxyfluorescein and TAMRA is 6-carboxytetramethylrhodamine). Reactions were performed on a CFX96 Touch real-time PCR detection system (Bio-Rad) and consisted of 15 min of initial denaturation at 95°C, followed by 50 thermal cycles of 15 s at 95°C and 40 s at 58°C. Standard curves were generated using 10-fold serial dilutions of known amounts of plasmid pGEM-T Easy containing the fragment amplified with the MAV-1 hexon forward and reverse primers. The thresholds were determined based on the results for the negative controls.

Quantification of MAV-1 specific antibodies by in-cell ELISA. 3T6 cells were plated in 96-well plates at 5 × 10³ cells per well, infected with 500 TCID₅₀ of MAV-1 per well, and incubated at 37°C in 5% CO₂. When a cytopathic effect was observed (at approximately 5 days p.i.), cells were fixed in 2% paraformaldehyde for 20 min at RT, washed 2 times in PBS, and blocked for 30 min with PBS, 10% FCS, 300 mM glycine. Cells were then incubated at 4°C for 2 h with mouse sera diluted 100-fold in the blocking solution. Cells were washed 3 times in PBS and incubated at room temperature for 30 min with a goat anti-mouse Ig polyclonal secondary antibody conjugated with alkaline phosphatase (0.5 µg/ml; Sigma). After 3 washes with PBS, *p*-nitrophenyl phosphate (Sigma) was added and the mixture was incubated for 1 h, and then the reaction was stopped with 1 M sodium hydroxide. The absorbance was read at 405 nm using a benchmark enzyme-linked immunosorbent assay plate reader (Thermo). Signals detected from mock-infected cells were used as the background, and this background was subtracted from the corresponding values obtained with MAV-1-infected wells.

Neutralization assay. Mouse sera were heat inactivated at 56°C for 30 min. BALF or sera were serially diluted in complete medium (2-fold dilutions from 1:4 to 1:256 or 1:64 to 1:16,384, respectively). These diluted serum/BALF samples were mixed with an equal amount of complete medium containing 2,000 TCID₅₀ of MAV-1 per ml and incubated for 1 h at 4°C. One hundred microliters of the virus-serum/BALF mixtures (eight replicates for each dilution) were added to 3T6 cells plated in 96-well plates at 5 × 10³ cells per well. The cells were incubated at 37°C in 5% CO₂, and the wells were monitored over 10 days for MAV-1 infection by immunofluorescence labeling. The antibody neutralizing titer corresponds to the inverse of the highest dilution at which infection was completely inhibited.

Histological analysis. Fixed lungs were put in xylene baths, and paraffin infiltration was performed in an automatic tissue sample processor. After embedding into paraffin blocks, 5-µm sections were cut, deparaffinized, and rehydrated in successive baths of xylene, absolute ethanol, 95% ethanol, 70% ethanol, and then PBS. Sections were routinely stained with hematoxylin and eosin and then examined by light microscopy.

Bronchoalveolar lavages. After euthanasia, the trachea was catheterized and BAL was performed by 2 consecutive flushes of the lungs with 1 ml ice-cold PBS containing cOMplete protease inhibitor cocktail (Roche). The cell density in BAL fluid (BALF) was evaluated using a hemocytometer after Tuerk solution staining (Sigma-Aldrich). Differential cell counts in BALF were determined by flow cytometry analysis.

Cell suspension preparations from organs. To harvest lung cells, mice were perfused with ice-cold PBS through the right ventricle. Then, lung lobes were collected into a C Tube (Miltenyi) containing complete Hanks balanced salt solution medium, 1 mg/ml collagenase D (Roche), and 50 µg/ml DNase I (Roche), processed with a gentleMACS dissociator (Miltenyi), and incubated for 30 min at 37°C. Suspensions of cells were washed, treated for lysis of the erythrocytes (red lysis buffer; eBioscience), and strained through a 70-µm-mesh-size filter.

Flow cytometry. Labeling of single-cell suspensions was performed in fluorescence-activated cell sorting (FACS) buffer (PBS containing 2 mM EDTA, 0.5% bovine serum albumin, and 0.1% NaN₃) at 4°C. Cells were first

incubated for 20 min with a purified rat IgG2a anti-mouse CD16/CD32 antibody (1/500) to block Fc binding. FACS staining was performed by using different panels of fluorochrome-conjugated antibodies against CD45 (clone 30-F11; phycoerythrin [PE]-Cy7; dilution, 1/200), major histocompatibility complex class II (MHC-II; clone M5/114.15.2; PE-Cy7; dilution, 1/2,000), CD3e (clone 145-2C11; allophycocyanin [APC]; dilution, 1/400), CD8 (clone 53-6.7; PE; dilution, 1/1,000), CD4 (clone RM 4-5; V450; dilution, 1/500), CD19 (clone MB19-1; APC-Cy7; dilution, 1/500), CD49b (clone DX5; fluorescein isothiocyanate; dilution, 1/500), Ly6G (clone 1A8; APC-Cy7; dilution, 1/500), CD11c (clone N418; Alexa Fluor 700; dilution, 1/500), CD11b (clone M1/70; Brilliant Violet 711; dilution, 1/1,500), Ly6C (clone HK1.4; BV785; dilution, 1/1,500), CD62L (clone MEL-14; eFluor 450; dilution, 1/1,000), and CD44 (clone IM7, PE-Cy7; dilution, 1/1,000). All antibodies were purchased from eBioscience, BD Biosciences, or BioLegend. Dead cells were stained using fixable viability stain 510 (BD Bioscience) or fixable viability dye eFluor 780 (eBioscience). Samples were analyzed on a BD LSR Fortessa X-20 flow cytometer equipped with 50-mW violet 405-nm, 50-mW blue 488-nm, 50-mW yellow-green 561-nm, and 40-mW red 633-nm lasers and an ND1.0 filter in front of the forward scatter (FSC) photodiode, using BD FACSDiva software. Data were analyzed with FlowJo software (TreeStar).

Statistical analysis. Data were analyzed with GraphPad Prism (version 5.0) software. For all the experiments, 5 mice were in each group. For weight curves, the data were analyzed by 2-way analysis of variance (ANOVA) and Bonferroni posttests. The qPCR data were analyzed by the Kruskal-Wallis method followed by Dunn's test. For serological analysis, we used the Wilcoxon-Mann-Whitney rank-sum test. For lung weights, the data were analyzed by 1-way ANOVA. For lung and BALF cellular populations, data were analyzed by 1-way ANOVA and Bonferroni posttests.

ACKNOWLEDGMENTS

E.G. is a research fellow of the Fund for Research Training in Industry and Agriculture (FRIA).

We thank the technician and administrative team of the laboratory of Immunology and Vaccinology ULiège for very helpful assistance. We thank Michel Bisteau and Philippe Hermand for their support in the design of the experiments and data analysis.

E.D. is an employee of the GSK group of companies and reports owning shares and/or restricted shares in GSK.

L.G., E.G., and B.M. designed the experiments with the help of E.D., C.D.P., and K.R.S.; E.G. and J.J. performed the experiments and compiled the data; E.G., L.G., B.M., and E.D. analyzed the data; E.G., B.M. and L.G. prepared the figures; E.G. and L.G. wrote the manuscript; all authors critically revised the manuscript for important intellectual content. All authors had full access to the data and approved the manuscript before it was submitted by the corresponding author.

This work was funded through a fellowship of the Fund for Research Training in Industry and Agriculture (FRIA) to E.G. through a VIR-IMPRINT ARC grant of the University of Liège and through a research collaboration agreement from GlaxoSmith-Kline Biologicals SA. K.R.S. and C.D.P. were supported by NIH NIAID R01AI091721 and R01AI133935.

REFERENCES

- Holmgren J, Czerkinsky C. 2005. Mucosal immunity and vaccines. *Nat Med* 11:S45–S53. <https://doi.org/10.1038/nm1213>.
- Neutra MR, Kozlowski PA. 2006. Mucosal vaccines: the promise and the challenge. *Nat Rev Immunol* 6:148–158. <https://doi.org/10.1038/nri1777>.
- Levine MM. 2010. Immunogenicity and efficacy of oral vaccines in developing countries: lessons from a live cholera vaccine. *BMC Biol* 8:129. <https://doi.org/10.1186/1741-7007-8-129>.
- Lycke N. 2012. Recent progress in mucosal vaccine development: potential and limitations. *Nat Rev Immunol* 12:592–605. <https://doi.org/10.1038/nri3251>.
- Dubois B, Goubier A, Joubert G, Kaiserlian D. 2005. Oral tolerance and regulation of mucosal immunity. *Cell Mol Life Sci* 62:1322–1332. <https://doi.org/10.1007/s00018-005-5036-0>.
- Sun M, He C, Cong Y, Liu Z. 2015. Regulatory immune cells in regulation of intestinal inflammatory response to microbiota. *Mucosal Immunol* 8:969–978. <https://doi.org/10.1038/mi.2015.49>.
- Khanal S, Ghimire P, Dhamoon A, Khanal S, Ghimire P, Dhamoon AS. 2018. The repertoire of adenovirus in human disease: the innocuous to the deadly. *Biomedicine* 6:E30. <https://doi.org/10.3390/biomedicine6010030>.
- Alexander J, Ward S, Mendy J, Manayani DJ, Farness P, Avanzini JB, Guenther B, Garduno F, Jow L, Snarsky V, Ishioka G, Dong X, Vang L, Newman MJ, Mayall T. 2012. Pre-clinical evaluation of a replication-competent recombinant adenovirus serotype 4 vaccine expressing influenza H5 hemagglutinin. *PLoS One* 7:e31177. <https://doi.org/10.1371/journal.pone.0031177>.
- Ahi YS, Bangari DS, Mittal SK. 2011. Adenoviral vector immunity: its implications and circumvention strategies. *Curr Gene Ther* 11:307–320. <https://doi.org/10.2174/156652311796150372>.
- Xiang ZQ, Gao GP, Reyes-Sandoval A, Li Y, Wilson JM, Ertl HC. 2003. Oral vaccination of mice with adenoviral vectors is not impaired by pre-existing immunity to the vaccine carrier. *J Virol* 77:10780–10789. <https://doi.org/10.1128/JVI.77.20.10780-10789.2003>.
- Deal C, Pekosz A, Ketner G. 2013. Prospects for oral replicating adenovirus-vectored vaccines. *Vaccine* 31:3236–3243. <https://doi.org/10.1016/j.vaccine.2013.05.016>.
- Crosby CM, Nehete P, Sastry KJ, Barry MA. 2015. Amplified and persistent immune responses generated by single-cycle replicating adenovirus vaccines. *J Virol* 89:669–675. <https://doi.org/10.1128/JVI.02184-14>.
- Top FH. 1975. Control of adenovirus acute respiratory disease in U.S. Army trainees. *Yale J Biol Med* 48:185–195.
- Barraza EM, Ludwig SL, Gaydos JC, Brundage JF. 1999. Reemergence of adenovirus type 4 acute respiratory disease in military trainees: report of an outbreak during a lapse in vaccination. *J Infect Dis* 179:1531–1533. <https://doi.org/10.1086/314772>.

15. Lyons A, Longfield J, Kuschner R, Straight T, Binn L, Seriwatana J, Reitstetter R, Froh IB, Craft D, McNabb K, Russell K, Metzgar D, Liss A, Sun X, Towle A, Sun W. 2008. A double-blind, placebo-controlled study of the safety and immunogenicity of live, oral type 4 and type 7 adenovirus vaccines in adults. *Vaccine* 26:2890–2898. <https://doi.org/10.1016/j.vaccine.2008.03.037>.
16. Hoke CH, Jr, Snyder CE, Jr. 2013. History of the restoration of adenovirus type 4 and type 7 vaccine, live oral (adenovirus vaccine) in the context of the Department of Defense acquisition system. *Vaccine* 31: 1623–1632. <https://doi.org/10.1016/j.vaccine.2012.12.029>.
17. Hoke CH, Jr, Hawksworth A, Snyder CE, Jr. 2012. Initial assessment of impact of adenovirus type 4 and type 7 vaccine on febrile respiratory illness and virus transmission in military basic trainees, March 2012. *MSMR* 19:2–4.
18. Kitchen LW, Vaughn DW. 2007. Role of U.S. military research programs in the development of U.S.-licensed vaccines for naturally occurring infectious diseases. *Vaccine* 25:7017–7030. <https://doi.org/10.1016/j.vaccine.2007.07.030>.
19. Tucker SN, Tingley DW, Scallan CD. 2008. Oral adenoviral-based vaccines: historical perspective and future opportunity. *Expert Rev Vaccines* 7:25–31. <https://doi.org/10.1586/14760584.7.1.25>.
20. Weaver EA. 2014. Vaccines within vaccines: the use of adenovirus types 4 and 7 as influenza vaccine vectors. *Hum Vaccin Immunother* 10: 544–556. <https://doi.org/10.4161/hv.27238>.
21. Kuschner RA, Russell KL, Abuja M, Bauer KM, Faix DJ, Hait H, Henrick J, Jacobs M, Liss A, Lynch JA, Liu Q, Lyons AG, Malik M, Moon JE, Stubbs J, Sun W, Tang D, Towle AC, Walsh DS, Wilkerson D, Adenovirus Vaccine Efficacy Trial Consortium. 2013. A phase 3, randomized, double-blind, placebo-controlled study of the safety and efficacy of the live, oral adenovirus type 4 and type 7 vaccine, in U.S. military recruits. *Vaccine* 31:2963–2971. <https://doi.org/10.1016/j.vaccine.2013.04.035>.
22. Lubeck MD, Davis AR, Chengalvala M, Natuk RJ, Morin JE, Molnar-Kimber K, Mason BB, Bhat BM, Mizutani S, Hung PP. 1989. Immunogenicity and efficacy testing in chimpanzees of an oral hepatitis B vaccine based on live recombinant adenovirus. *Proc Natl Acad Sci U S A* 86:6763–6767. <https://doi.org/10.1073/pnas.86.17.6763>.
23. Gurwith M, Lock M, Taylor EM, Ishioka G, Alexander J, Mayall T, Ervin JE, Greenberg RN, Strout C, Treanor JJ, Webby R, Wright PF. 2013. Safety and immunogenicity of an oral, replicating adenovirus serotype 4 vector vaccine for H5N1 influenza: a randomised, double-blind, placebo-controlled, phase 1 study. *Lancet Infect Dis* 13:238–250. [https://doi.org/10.1016/S1473-3099\(12\)70345-6](https://doi.org/10.1016/S1473-3099(12)70345-6).
24. Tacket CO, Lososky G, Lubeck MD, Davis AR, Mizutani S, Horwith G, Hung P, Edelman R, Levine MM. 1992. Initial safety and immunogenicity studies of an oral recombinant adenohepatitis B vaccine. *Vaccine* 10: 673–676. [https://doi.org/10.1016/0264-410X\(92\)90088-2](https://doi.org/10.1016/0264-410X(92)90088-2).
25. Ginsberg HS, Moldawer LL, Sehgal PB, Redington M, Kilian PL, Chanock RM, Prince GA. 1991. A mouse model for investigating the molecular pathogenesis of adenovirus pneumonia. *Proc Natl Acad Sci U S A* 88:1651–1655. <https://doi.org/10.1073/pnas.88.5.1651>.
26. Pacini DL, Dubovi EJ, Clyde WA. 1984. A new animal model for human respiratory tract disease due to adenovirus. *J Infect Dis* 150:92–97. <https://doi.org/10.1093/infdis/150.1.92>.
27. Hjorth RN, Bonde GM, Pierzchala WA, Vernon SK, Wiener FP, Levner MH, Lubeck MD, Hung PP. 1988. A new hamster model for adenoviral vaccination. *Arch Virol* 100:279–283. <https://doi.org/10.1007/BF01487691>.
28. Spindler KR, Fang L, Moore ML, Hirsch GN, Brown CC, Kajon A. 2001. SJL/J mice are highly susceptible to infection by mouse adenovirus type 1. *J Virol* 75:12039–12046. <https://doi.org/10.1128/JVI.75.24.12039-12046.2001>.
29. Weinberg JB, Jensen DR, Gralinski LE, Lake AR, Stempfle GS, Spindler KR. 2007. Contributions of E1A to mouse adenovirus type 1 pathogenesis following intranasal inoculation. *Virology* 357:54–67. <https://doi.org/10.1016/j.virol.2006.08.013>.
30. Weinberg JB, Stempfle GS, Wilkinson JE, Younger JG, Spindler KR. 2005. Acute respiratory infection with mouse adenovirus type 1. *Virology* 340:245–254. <https://doi.org/10.1016/j.virol.2005.06.021>.
31. Adkins LJ, Molloy CT, Weinberg JB. 2018. Fas activity mediates airway inflammation during mouse adenovirus type 1 respiratory infection. *Virology* 521:129–137. <https://doi.org/10.1016/j.virol.2018.06.002>.
32. McCarthy MK, Zhu L, Procario MC, Weinberg JB. 2014. IL-17 contributes to neutrophil recruitment but not to control of viral replication during acute mouse adenovirus type 1 respiratory infection. *Virology* 456–457: 259–267. <https://doi.org/10.1016/j.virol.2014.04.008>.
33. McCarthy MK, Malitz DH, Molloy CT, Procario MC, Greiner KE, Zhang L, Wang P, Day SM, Powell SR, Weinberg JB. 2016. Interferon-dependent immunoproteasome activity during mouse adenovirus type 1 infection. *Virology* 498:57–68. <https://doi.org/10.1016/j.virol.2016.08.009>.
34. Procario MC, Levine RE, McCarthy MK, Kim E, Zhu L, Chang C-H, Hershenson MB, Weinberg JB. 2012. Susceptibility to acute mouse adenovirus type 1 respiratory infection and establishment of protective immunity in neonatal mice. *J Virol* 86:4194–4203. <https://doi.org/10.1128/JVI.06967-11>.
35. Wigand R. 1980. Age and susceptibility of Swiss mice for mouse adenovirus, strain FL. *Arch Virol* 64:349–357. <https://doi.org/10.1007/BF01320620>.
36. Guida JD, Fejer G, Pirofski LA, Brosnan CF, Horwitz MS. 1995. Mouse adenovirus type 1 causes a fatal hemorrhagic encephalomyelitis in adult C57BL/6 but not BALB/c mice. *J Virol* 69:7674–7681.
37. Kajon AE, Brown CC, Spindler KR. 1998. Distribution of mouse adenovirus type 1 in intraperitoneally and intranasally infected adult outbred mice. *J Virol* 72:1219–1223.
38. Zhang J, Kang J, Dehghan S, Sridhar S, Lau SKP, Ou J, Woo PCY, Zhang Q, Seto D. 2019. A survey of recent adenoviral respiratory pathogens in Hong Kong reveals emergent and recombinant human adenovirus type 4 (HAdV-E4) circulating in civilian populations. *Viruses* 11:E129. <https://doi.org/10.3390/v11020129>.
39. Wang B, Li J, Wu S, Chen Y, Zhang Z, Zhai Y, Guo Q, Zhang J, Song X, Zhao Z, Hou L, Chen W. 2018. Seroepidemiological investigation of HAdV-4 infection among healthy adults in China and in Sierra Leone, West Africa. *Emerg Microbes Infect* 7:200. <https://doi.org/10.1038/s41426-018-0206-y>.
40. Hilleman MR, Werner JH. 1954. Recovery of new agent from patients with acute respiratory illness. *Proc Soc Exp Biol Med* 85:183–188. <https://doi.org/10.3181/00379727-85-20825>.
41. Dehghan S, Seto J, Liu EB, Walsh MP, Dyer DW, Chodosh J, Seto D. 2013. Computational analysis of four human adenovirus type 4 genomes reveals molecular evolution through two interspecies recombination events. *Virology* 443:197–207. <https://doi.org/10.1016/j.virol.2013.05.014>.
42. Hoppe E, Pauly M, Gillespie TR, Akoua-Koffi C, Hohmann G, Fruth B, Karhemere S, Madinda NF, Mugisha L, Muyembe JJ, Todd A, Petzelkova KJ, Gray M, Robbins M, Bergl RA, Wittig RM, Zuberbühler K, Boesch C, Schubert G, Leendertz FH, Ehlers B, Calvignac-Spencer S. 2015. Multiple cross-species transmission events of human adenoviruses (HAdV) during hominine evolution. *Mol Biol Evol* 32:2072–2084. <https://doi.org/10.1093/molbev/msv090>.
43. Zhu Z, Zhang Y, Xu S, Yu P, Tian X, Wang L, Liu Z, Tang L, Mao N, Ji Y, Li C, Yang Z, Wang S, Wang J, Li D, Xu W. 2009. Outbreak of acute respiratory disease in China caused by B2 species of adenovirus type 11. *J Clin Microbiol* 47:697–703. <https://doi.org/10.1128/JCM.01769-08>.
44. Kesiosoglou F, Schmiedlin-Ren P, Fleisher D, Zimmermann EM. 2010. Adenoviral transduction of enterocytes and M-cells using in vitro models based on Caco-2 cells: the coxsackievirus and adenovirus receptor (CAR) mediates both apical and basolateral transduction. *Mol Pharm* 7:619–629. <https://doi.org/10.1021/mp9001377>.
45. Renegar KB, Small PA, Jr, Boykins LG, Wright PF. 2004. Role of IgA versus IgG in the control of influenza viral infection in the murine respiratory tract. *J Immunol* 173:1978–1986. <https://doi.org/10.4049/jimmunol.173.3.1978>.
46. Beard CW, Spindler KR. 1996. Analysis of early region 3 mutants of mouse adenovirus type 1. *J Virol* 70:5867–5874.
47. Cauthen AN, Brown CC, Spindler KR. 1999. In vitro and in vivo characterization of a mouse adenovirus type 1 early region 3 null mutant. *J Virol* 73:8640–8646.
48. Smith K, Ying B, Ball AO, Beard CW, Spindler KR. 1996. Interaction of mouse adenovirus type 1 early region 1A protein with cellular proteins pRb and p107. *Virology* 224:184–197. <https://doi.org/10.1006/viro.1996.0520>.
49. Reed LJ, Muench H. 1938. A simple method of estimating fifty percent endpoints. *Am J Epidemiol* 27:493–497. <https://doi.org/10.1093/oxfordjournals.aje.a118408>.